Desalination and Water Treatment
www.deswater.com
doi: 10.1080/19443994.2013.803769

52 (2014) 2905–2919
April

Taylor & Francis
Taylor & Francis Group

Hybrid thermal–thermal desalination structures

Gina M. Zak, Alexander Mitsos*

Department of Mechanical Engineering, Massachusetts Institute of Technology, 77 Massachusetts Avenue, Cambridge, MA 02139, USA
Email: amitsos@alum.mit.edu

Received 12 July 2012; Accepted 23 April 2013

ABSTRACT

Opportunities exist to improve industrial-scale thermal desalination system performance and reliability through novel process structures. Herein, hybrid thermal–thermal desalination structure concepts that combine the merits of MSF, MED, or MED-TVC are proposed. The first is a system which transitions from forward-feed MED effects to parallel-cross MED effects (FF-PC-MED) and could be combined with TVC (FF-PC-MED-TVC). The second is a system which transitions from MSF stages to forward-feed MED effects (MSF-MED) and employs a vapor routing for MSF which typically not used. Finally, the last system uses parallel steam supplies to power MSF stages and MED-TVC effects configured in series (MSF-MED-TVC). Through the simulation of their performance, it is found that these concepts can exhibit higher performance ratio and/or lower specific heat transfer surface area as compared to standard thermal desalination configurations for fixed operating conditions. While these results indicate that the hybrid thermal–thermal desalination structures are promising alternatives to standard thermal desalination configurations, detailed modeling, and numerical optimization of the concepts is necessary in future work.

Keywords: MSF; MED; Thermal desalination; Structural optimization; Optimal design

1. Introduction

Industrial-scale thermal desalination technologies involve evaporative processes and, in general, are highly energy-intensive with high capital and operating costs. As such, since their development in the early- and mid-twentieth century, many different technologies have been developed to reduce energy consumption and economic investment. The main types of industrial-scale thermal desalination are multi-stage flash (MSF) and multi-effect distillation (MED), and each has several configurations. For MSF, the most common configurations are once-through (OT), brine mixing, or brine-recirculation (BR) [1]. For MED, the most common configurations are parallel feed, forward-feed (FF), parallel-cross (PC), and backward-feed with or without thermal vapor compression (TVC) [2,3]. Each of these technologies has performance trade-offs in thermal efficiency, capital costs, operating costs, and reliability. Currently, the most commonly installed technology is the MSF-BR system because of its proven reliability and large capacity [4]. However, MED and MED-TVC are gaining attention due to higher thermal efficiency and the potential for lower steam supply temperatures [5–7].

Despite the many existing thermal desalination configurations, alternative configurations could prove to exhibit better performance. Some authors have

*Corresponding author.

investigated the gain in thermal efficiency, reduction in heat transfer areas, gain in reliability, or reduction in costs, with alternative routings of feed, brine, or distillate and combinations of hardware.

Nafey et al. [8] utilize exergetic and thermoeconomic analyses to develop a hybrid MED-MSF system where a portion of the brine of an MSF stage is utilized as feed to an MED effect. Nafey et al. cite a reduction in specific cost of water as compared to MSF-BR, FF-MED with feedwater heaters (FWH), and PC-MED without FWH. However, El-Dessouky and Ettouney [9] show that PC-MED with FWH exhibits higher performance for fixed number of effects and operating conditions as compared to FF-MED with FWH. Therefore, the hybrid MSF-MED proposed in [8] should also be compared to PC-MED with FWH.

Sommariva et al. investigate the routing of distillate in MSF systems [10–12]. Sommariva et al. thermodynamically model and experimentally confirm that extracting distillate from MSF stages leads to higher distillate production. Further, according to Sommariva et al., the extracted distillate can be utilized for secondary processes which inform the addition of a distillate-to-brine heat exchanger [10] and the possibility of a hybrid MSF-MED scheme where the extracted distillate is utilized to power MED effects [11,13].

Mussati et al. utilize a numerical approach to structurally optimize MSF systems [14–16]. This work is based partially on the work by Scenna [17,18], who approached the numerical optimization of MSF and MED structures as a heat exchanger network problem. In [14], Mussati et al. present a superstructure (expanded in [15,16]) for MSF configurations which allows routing possibilities for distillate extraction and feed and recycle streams. A heuristic algorithm is used for optimization where a simplified, nonrigorous model is solved before solving the full optimization problem. Mussati et al. do not consider the possibility of utilizing other evaporation methods, e.g., boiling, to construct an optimal thermal desalination configuration.

The previous work investigating alternative thermal desalination structures elucidates the opportunities for the improvement of industrial-scale thermal desalination. The configuration of brine, feed, and/or distillate as well as use of flashing and/or boiling to generate salt-free vapor all have implications on a thermal desalination system's potential thermal performance and operating costs. The aim of this article is to propose alternative thermal desalination structural concepts, specifically, hybrid thermal–thermal desalination structures, which draw upon the merits of standard thermal desalination configurations. The simulation results serve as proof of concept and to demonstrate the need for detailed modeling and numerical optimization. The structures proposed are special cases of a superstructure proposed in [19].

2. Thermal desalination configurations

Hybrid thermal–thermal desalination concepts are explored herein. The first concept demonstrates the performance trade-offs between FF-MED and PC-MED by investigating a concept which refers to transitions from the FF to PC configuration within a given number of effects. The additional proposed concepts are combinations of MSF and MED configurations, which are different than those proposed in [11,13,20] since brine and vapor of MSF are used directly for the MED section. One concept combines MSF with FF-MED and demonstrates an alternate vapor routing from an MSF stage. The last concept combines MSF and FF-MED-TVC with parallel steam supplies. For more information on the standard MSF and MED (-TVC) configurations, see [21–23].

This study measures the performance of alternative structures in terms of performance ratio (PR, the ratio of distillate flow rate to input steam flowrate), recovery ratio (RR, the percentage of distillate produced to the total feed flowrate), and specific heat transfer surface area (SA, the ratio of heat transfer surface area to distillate production) as compared to standard thermal desalination configurations. PR and RR are measures of operating costs and SA is a measure of capital costs [21]. It is desired that PR and RR are maximized, while SA is minimized. Weighing the performance of different configurations constitutes trade-offs between these competing objectives.

The steam supply conditions for thermal desalination also impact the performance of a dual-purpose power and water co-generation system (typical on the industrial-scale when utilizing thermal desalination). Greater steam supply temperatures for thermal desalination result in greater loss of electrical work per unit of steam extracted from the power cycle as compared to lower steam supply temperatures. Since most industrial-scale thermal desalination plants are integrated with power cycles, it is important to consider this trade-off in electricity production with varying steam supply conditions. However, herein, the proposed thermal desalination concepts are compared against standard configurations with the same steam supply conditions, e.g., a nonstandard configuration compared against MSF will use a steam supply temperature of ≈110–120°C, and a nonstandard configuration compared against MED will use a steam supply temperature of ≈70–80°C. Therefore, the objective of maximizing PR also minimizes its impact to a coupled power cycle for constant water production. This

simplification enables the consideration of only the thermal desalination plant performance.

2.1. Forward to parallel-cross MED

The first configuration considered is a hybrid between FF-MED and PC-MED (FF-PC-MED). For a given number of total effects, N_t, the feed switches from FF to PC at effect N_s. Fig. 1 shows a depiction of the FF-PC-MED concept. The total feed is preheated in FWH along the effects. In the PC section, part of the total feed is directed to each effect. At effect N_s, the remaining feed is directed to effect 1. In the FF section, the brine from the previous effect is directed as feed in the next effect. In the PC section, the brine from the previous effect is flashed and mixed with the brine of the next effect. The distillate from each effect is flashed and mixed with the distillate of the next effect.

The primary motivation for exploring FF-PC-MED is the trade-off in PR and SA that exists between FF-MED and PC-MED. In particular, for fixed operating temperatures, maximal allowed brine salinity, and number of effects, PC-MED has a higher PR but also a higher SA as compared to FF-MED (shown in more detail later). It is expected that the FF-PC-MED configuration exhibits intermediate PR and SA as compared to FF-MED and PC-MED under the same operating conditions and number of effects. However, it will be shown that for a given PR, the FF-PC-MED requires less SA than any linear combination of purely FF-MED and PC-MED systems.

The linear combination is a fleet-level performance measure for alternative systems in the presence of multiple objectives [24,25]. In particular, a hybrid system of two existing technologies must be able to exhibit better performance than a combination of plants which could be built by the existing technologies alone. Otherwise, the hybrid concept is not competitive on the fleet level. In this context, both the PR and SA are independent of total distillate mass flowrate for fixed temperatures, recovery, and number of effects. Therefore, a linear combination of FF-MED and PC-MED plants can be used to achieve an intermediate overall PR and SA for fixed number of effects and operating conditions as compared to either FF-MED or PC-MED alone.

It is important to note that the effects of the FF section in FFPC-MED have higher brine temperature than the effects of the PC section, since they are closest to the steam supply. This design choice (as opposed to the PC section being closest to the steam supply) is motivated by the gradual increase in brine salinity along effects which is characteristic of FF-MED. With the FF effects, the lowest brine salinities are at the highest temperatures, which is an operational advantage as compared to PC-MED alone. In PC-MED, the maximum brine salinity is reached in each effect. Therefore, a greater risk for scaling in the high-temperature effects of PC-MED is present in comparison to FF-PC-MED [2].

The FF-PC-MED concept could also be utilized with TVC. As compared to FF-PC-MED alone, a higher PR can be achieved with TVC at the expense of a higher steam supply temperature/pressure (for fixed number of effects and top brine temperature (TBT)). However, FF-PC-MED with TVC is not analyzed herein because the main interest of this study is the performance effect of the brine- and feed-routing transition between FF and PC. The relative performance gain of FF-PC-MED as compared to FF-MED or PC-MED for fixed operating conditions and number of effects would also exist for FF-PC-MED with TVC as compared to FF-MED-TVC or PC-MED-TVC for fixed TVC design.

2.2. MSF to forward-feed MED or forward-feed MED-TVC

The second structural concept involves the combination of MSF and FF-MED in series, referred to hereafter as MSF-MED. The configuration is comprised of a section of MSF stages in series with a

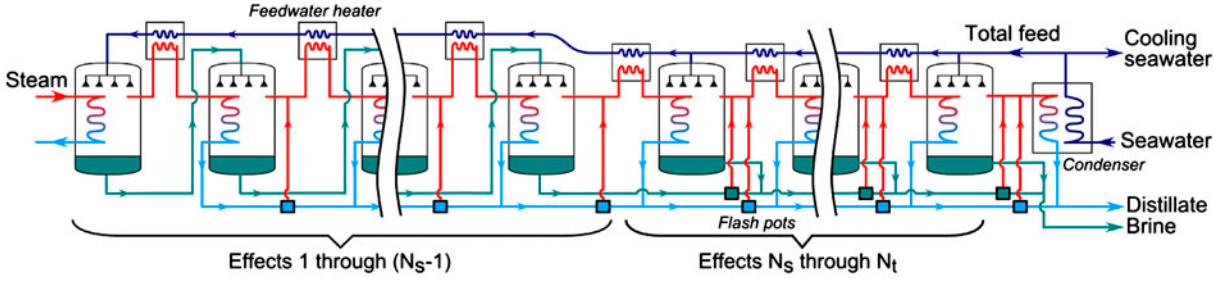

Fig. 1. Forward to parallel-cross MED concept (FF-PC-MED) with N_t total number of effects and transition from forward-feed to parallel-cross configuration at effect N_s.

section of MED effects. The brine of the last MSF stage is directed as feed of the first MED effect. In addition, the vapor produced in the last MSF stage is used to power the first MED effect. In a typical MSF stage, the flashed vapors are condensed on the outside of tubes in order to raise the temperature of feedwater. However, in the MSF-MED concept, unit $N_s - 1$ constitutes a mechanical construct other than an MSF stage or MED effect, i.e., the flashed vapors of unit $N_s - 1$ are directed to condense inside of tubes to power the first MED effect. A motivation for investigating the MSF-MED configuration is to determine if there is merit in utilizing this alternate unit type. Fig. 2 shows the MSF-MED concept; the structure transitions to FF-MED at unit N_s. The total feed is preheated along both the MED and MSF sections.

The third structural concept combines MSF with FF-MED-TVC, referred to hereafter as MSF-MED-TVC. This configuration is similar to the previous case, but TVC is used to power the first MED effect. A motivation for investigating this configuration is the common steam supply temperature that is possible for TVC motive steam and steam supply to the MSF brine heater. Fig. 3 shows the MSF-MED-TVC concept. The total feed is preheated along both the MED and MSF effects and directed to the first MSF stage.

It is important to note that seawater pretreatment to prevent scaling of seawater constituents, in particular $CaSO_4$ (whose solubility is dependent on both temperature and salinity), is typically different in standalone MSF as compared to standalone MED due to differences in their operating range [26]. Therefore, for practical implementation of the MSF-MED or MSF-MED-TVC concepts, investigation of economically feasible and reliable pretreatment methods would be necessary for direct use of MSF brine as MED feed. Further, in standalone MED, the TBT is limited to ≈65–70°C in order to avoid scaling in the evaporators [6]. This heuristic temperature limitation informs the operation and design of the MSF-MED and MSF-MED-TVC concepts as well. Discussed in more detail later, the transition unit N_s for fixed total units in MSF-MED and the entrainment ratio for TVC with fixed steam supply temperature/pressure of MSF-MED-TVC are constrained by the maximum recommended brine temperature of an MED effect.

3. Thermodynamic modeling of processes

Each of the concepts utilizes combinations of the physical processes involved in standard thermal desalination structures, namely evaporation by flashing, evaporation by film boiling, condensation, preheat, mixing, and thermal vapor compression. As such, these processes can be modeled from a control volume perspective and combined to reflect specific thermal desalination configurations. In this section, First Law control-volume models of these processes are shown that are common in the literature [2,22,27–30]. Additional considerations, e.g., the effect of demisters,

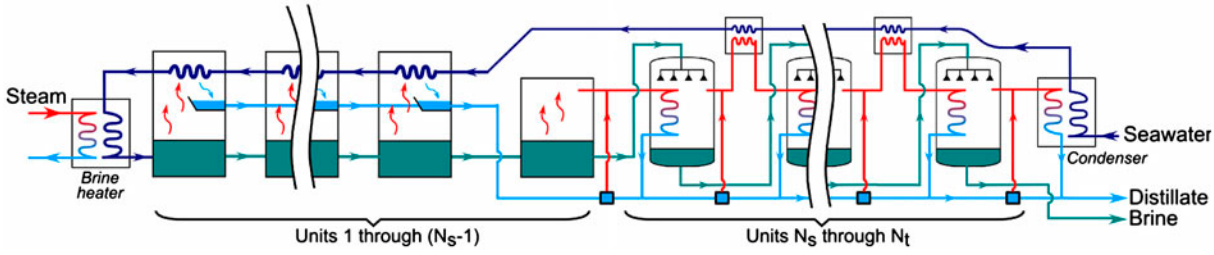

Fig. 2. MSF to FF-MED concept with alternative vapor routing of MSF for unit $N_s - 1$.

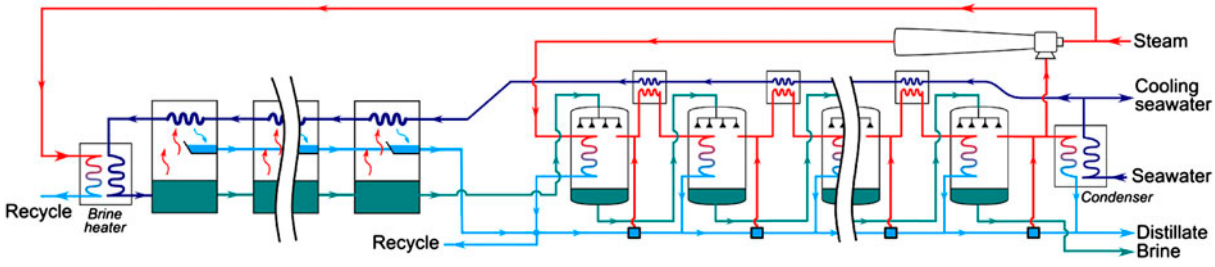

Fig. 3. MSF-MED-TVC concept with parallel steam supplies.

noncondensable gases, de-superheaters, fouling resistances, and/or nonequilibrium allowances [31–35], could be included in performance estimations. However, their calculation requires detailed knowledge of process geometry. Further, since the goal of this article is to demonstrate the merit of the proposed concept configurations, these additional considerations are neglected herein.

The working fluids involved in thermal desalination include pure water (distillate), water vapor, and water containing dissolved salts (brine and feedwater). It is assumed that water vapor, and hence distillate is also salt-free. The effect of noncondensable gases is neglected herein. Simplified physical properties are utilized in the models which, for the purpose of this article, are sufficient. No claim for the thermodynamic consistency of the models is made. Constant enthalpy of vaporization and specific heat capacity are assumed as 2,333 kJ/kg and 4 kJ/(kg K), respectively. The effect of pressure is neglected in the calculation of enthalpy; therefore, $\Delta h = c_p \Delta T$. These assumptions are common in the thermal desalination modeling literature [9,22,36]. A common assumption in the literature is a constant temperature drop to account for boiling point elevation (BPE). In contrast, herein, the BPE is accounted for by empirical correlations (discussed later) because of sensitivity of heat transfer area calculations with respect to the accuracy of BPE calculation [28].

In unit models which interface with external steam supply (first effect/stage condenser and TVC), the 1997 IAPWS Industrial Formulation for pure water [37] is utilized to capture the effect of steam supply pressure. The purpose of utilizing this formulation is to coincide with typical power production modeling where the use of IAPWS properties is customary (though it is not essential for the purposes herein). Physical property formulations which are less exact (and less computationally expensive) than the IAPWS formulation could be utilized without substantial loss of accuracy.

Evaporation of water is the main goal of thermal desalination and can occur by flashing or film boiling. In the case of flashing, typically, there is no heat input. In the case of film boiling, evaporation is mainly due to heat input. Therefore, based on the physical property assumptions made herein, the energy balance of evaporation is given by:

$$\dot{Q} = \dot{m}_f c_p (T_b - T_f) + \dot{m}_v \Delta h_{fg}$$

where $\dot{m}_f$ is the feed mass flow rate, T_f is the feed temperature, $\dot{m}_v$ is the mass flow rate of the produced vapor, T_b is the temperature of the outlet brine, Δh_{fg} is the enthalpy of vaporization of the seawater, and c_p is the specific heat capacity. In the case of flashing, $\dot{Q} = 0$. The mass balance is given by $m_f = \dot{m}_b + \dot{m}_v$. It should be noted that in the case of film boiling, if the saturated pressure of the feed is greater than the brine saturation pressure ($P_{f,sat} \geq P_{b,sat}$), then part of the formed vapor is generated by flashing [22].

The heat transfer area required for film boiling is given by:

$$A = \frac{\dot{Q}}{U(T_q - T_b)}$$

where T_q is the temperature of the heat input, U is the overall heat transfer coefficient, and A is the heat transfer area, assuming a well-mixed control volume. In this work, the overall heat transfer coefficient is taken as a constant $U = 3$ kW/(m^2 K) [22]. Taking the overall heat transfer coefficient as constant limits the accuracy of heat transfer area calculations. The heat transfer coefficient tends to increase with increasing temperature. However, since the overall structure is the main consideration herein (which influences the possible operating temperatures of the plant and thus, the $T_q - T_b$ term, this loss of accuracy is acceptable for a gain in computational simplicity. Considering the possible tube geometries and flow velocities associated with the boiling process would be needed in order to accurately model the SA requirement.

The generated vapor from evaporation is superheated due to boiling point elevation of the seawater. After condensation, the temperature of the distillate is

$$T_d = T_b - BPE(T, X)$$

where BPE is the boiling point elevation of the brine and X is salinity of the brine. The BPE is calculated by correlations provided by [38] as a function of temperature and salinity:

$$BPE = A(X \times 10^{-3})^2 + B(X \times 10^{-3})$$

$$A = (-4.584 \times 10^{-4})T^2 + (2.823 \times 10^{-1})T + 17.95$$

$$B = (1.536 \times 10^{-4})T^2 + (5.267 \times 10^{-2})T + 6.56$$

The BPE calculations are valid for $0<T<200$°C and $0<X<0.12$ kg/kg accuracy of ±0.018°C.

Since the generated vapor of the evaporation processes is considered salt-free, species balance for both flash and film boiling is simply given by:

$$\dot{m}_b X_b = \dot{m}_f X_f$$

where X_b and X_f are the salinities of the brine and feed, respectively.

Condensation of water vapor outside or inside of tubes is associated with a heat output. Although the generated vapor is superheated, it is assumed that the difference in enthalpy between the generated vapor and saturated vapor at the distillate temperature is negligible. Further, it is assumed that there is no pressure drop. Therefore, energy balance of the condensation process is simply given by:

$$\dot{Q} = \dot{m}\Delta h_{fg}$$

Preheat of feedwater is modeled herein as a one-sided heat exchanger with a heat input. In the context of a thermal desalination plant, this process occurs in the feedwater heaters or end condenser in MED or the tube bundles of MSF. The energy balance of preheating based on the physical property assumptions is given by:

$$\dot{Q} = \dot{m}c_p(T_o - T_i)$$

where T_i and T_o are the inlet and outlet temperature of the feedwater being preheated, respectively. In order to estimate the heat transfer area, the ϵ-NTU method is utilized [39] with constant overall heat transfer coefficient of $U = 2.4\ \mathrm{kW/(m^2\ K)}$ [2]. Also, it is assumed that the heat input is produced by a two-phase process (condensation) which is a constant temperature.

The mass, energy (based on physical property assumptions), and species balance of mixing are as follows:

$$\dot{m}_o = \sum_{j=1}^{n} \dot{m}_j$$

$$\dot{m}_o T_o = \sum_{j=1}^{n} \dot{m}_j T_j$$

$$\dot{m}_o X_o = \sum_{j=1}^{n} \dot{m}_j X_j$$

where n is the number of inlet streams.

Thermal vapor compression uses high-pressure steam to entrain a low-pressure vapor. TVC involves a nozzle, mixer, and diffuser with supersonic flows [40]. The mass balance of the TVC is given by:

$$\dot{m}_e + \dot{m}_m = \dot{m}_{di}$$

where subscript "e" is the entrained stream, subscript "m" is the motive stream, and subscript "di" is the discharged stream. The ratio of mass flowrate of motive steam to entrained vapor, i.e., the entrainment ratio, is dependent on the design of the TVC. In order to estimate the TVC performance, the following correlation is utilized [21]:

$$\begin{aligned} ER &= \frac{\dot{m}_m}{\dot{m}_e} \\ &= 0.296 \times \frac{(P_{di})^{1.19}}{(P_e)^{1.04}} \\ &\quad \times \left(\frac{P_m}{P_e}\right)^{0.015} \times \left(\frac{3 \times 10^{-7}(P_m)^2 - 0.0009(P_m) + 1.6101}{2 \times 10^{-8}(T_e)^2 - 0.0006(T_e) + 1.0047}\right) \end{aligned}$$

where P_m, P_{di}, and P_e are in kPa and T_e is in ℃. According to El-Dessouky and Ettouney, this correlation agrees to within 10% of manufacturer's data over the following ranges: $ER \leq 4.5$, $10 < T_e \leq 500°C$, $100 \leq P_m \leq 3,500$ kPa, and $\frac{P_{di}}{P_e} \geq 1.81$.

The discharged stream is at an intermediate pressure as compared to the motive and entrained streams, which is typically chosen by the compression ratio (CR), i.e., the ratio of discharge pressure to entrained pressure. Finally, assuming an adiabatic process, the energy balance is given by:

$$\dot{m}_{di} h_{di} = \dot{m}_e h_e + \dot{m}_m h_m$$

As noted earlier, the TVC process interfaces with power plant steam supply and therefore, nonsimplified physical properties are used.

The above equations are utilized to describe control volumes whose inlet and outlet streams are connected in order to describe a particular thermal desalination configuration. Fig. 4 illustrates this approach for a single stage of MSF and single effect of parallel-cross MED. In the case of MSF (Fig. 4(a)), the control volumes involved are evaporation by flashing, condensation, and preheating (whose energy and mass balances are described by the above equations). The material streams are brine, distillate, feed and vapor that, based on the modeling assumptions, have

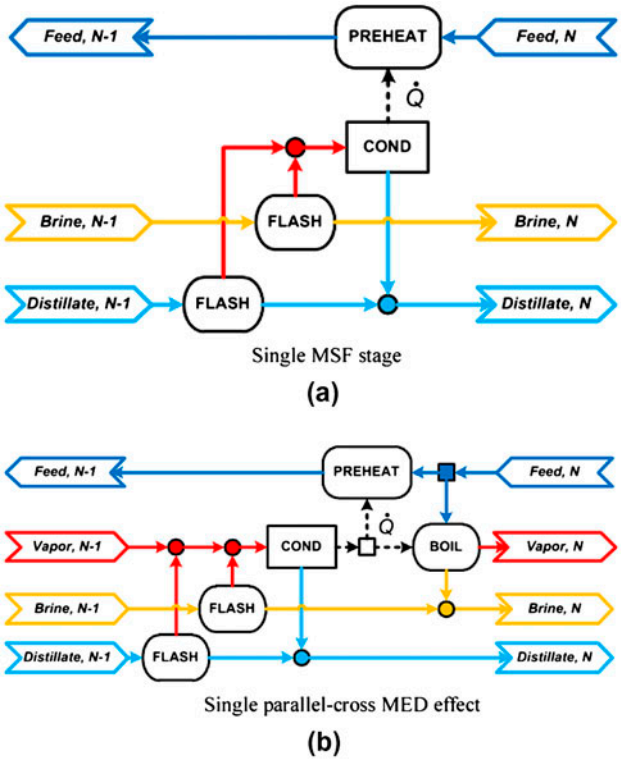

Fig. 4. Example for connectivity of MSF stage and parallel-cross MED effect utilizing process control volume approach.

an associated temperature, mass flow, and salinity (which may be equal to zero). Heat transfer is described by a stream with an associated flowrate and temperature (labeled by $\dot{Q}$). This connectivity is repeated with varying operating conditions in order to describe an entire once-through MSF plant. Similarly, Fig. 4(b) illustrates the control volume connectivity for the representation of parallel-cross MED. In this case, evaporation by film boiling is present.

The control volume approach utilized herein facilitates the simulation of thermal desalination systems. Ultimately, the connectivity of these control volumes defines a particular thermal desalination configuration. Therefore, the simulation of the configurations discussed hereafter are constructed by defining the connectivity of relevant control volumes and specifying operating conditions in order to estimate performance.

4. Simulation of concept performance and discussion

In this section, the performance of the hybrid thermal–thermal desalination concepts is simulated and compared vs. standard thermal desalination configurations, namely MED, MED-TVC, and/or MSF. The control volume models discussed in the previous section are utilized to simulate the performance after appropriately connecting the brine, feed, vapor, and distillate streams. The results of these simulations are utilized to elucidate the potential benefits of these concepts and identify areas where further investigation through detailed modeling is necessary.

4.1. Simulation and discussion of FF-PC-MED

The FF-PC-MED concept is compared to standalone FF-MED and PC-MED in order to determine if a performance advantage exists over the standard configurations; the aforementioned linear combination metric involving PR and SA is of particular interest. As a first step in this comparison, the performance of FF-MED and PC-MED with FWH is simulated utilizing the thermodynamic process models discussed in the previous section implemented in JACOBIAN differential algebraic equation software [41]. Each system is operated under the conditions shown in Table 1 and are near typical operating conditions of the literature [2,20,22]. The number of effects is variable, and it is assumed that the brine temperature drop between effects is constant. Therefore, the brine temperature profile is linear and described by:

$$\Delta T = \frac{TBT - T_{bd}}{N_t - 1}$$

where TBT is the top brine temperature (brine temperature of the first effect), T_{bd} is the brine blowdown temperature (brine temperature of the last effect), and N_t is the total number of effects. A linear temperature profile is a common assumption in the literature [22,35,42]. It is also assumed that the temperature rise in the FWH is equal to the drop temperature drop between effects (ΔT) The calculation of BPE is evaluated at the exit of each effect.

The total feed flowrate of each case is determined based on the required distillate flow (100 kg/s) and the maximum allowed brine salinity (72 g/kg). In the

Table 1
Operating parameters for PC-MED, FF-MED, and FF-PC-MED

Unit distillate flow (kg/s)	100
Seawater temperature (°C)	25
Seawater salinity (g/kg)	42
Max. brine salinity (g/kg)	72
Steam supply temp., saturated (°C)	70
Top brine temp., TBT (°C)	65
Brine blowdown temp., T_{bd} (°C)	40
Condenser temperature (°C)	35

case of FF-MED, where the total feed is directed to the first effect, the total feed is determined such that the brine salinity exiting the last effect is the maximum brine salinity given the required distillate flow. In the case of PC-MED, the total feed is split among the effects, and therefore, the feed to each effect is determined by setting the brine salinity after brine flashing to the maximal brine salinity. Since the feed is chosen such that the maximal brine salinity is achieved for both FF-MED and PC-MED, the RR of each system is the same (RR = 41.7%) and the maximum allowed (given the heuristic constraint to avoid scaling).

Tables 2 and 3 show simulation results for twelve effect FF-MED and PC-MED, respectively. The parameter $\dot{m}_v$ is the total vapor generated by the effect (including brine and distillate flashing). The distillate temperatures, T_d, are different between FF-MED and PC-MED despite setting the same brine temperatures. This difference is due to the variation in brine salinity which affects the BPE and thus the distillate temperature. The SA is the sum of evaporator, FWH, and down condenser heat transfer surface areas vs. the total mass flow rate of distillate produced.

The FF-MED achieves a PR of 9.47 with a SA of 439 $m^2/(kg/s)$. The PC-MED achieves a PR of 10.3 with a SA of 524 $m^2/(kg/s)$. These results illustrate the trade-off in PR and SA between FF-MED and PC-MED configurations.

Next, the operating conditions shown in Table 1 are utilized to simulate FF-PC-MED system. The total number of effects, N_t, and the effect where the configuration switches from FF to PC, N_s, are variable. As with FF-MED and PC-MED, the temperature drop across effects and temperature rise in the FWH is assumed constant. The feed of the system is determined by

Table 2
Forward-feed MED results. 12 effects, PR = 9.47, SA = 439 $m^2/(kg/s)$, and area of down condenser = 1,010 m^2

Effect	T_b	T_d	T_f	$T_{i,FWH}$	$\dot{m}_f$	$\dot{m}_v$	$\dot{m}_b$	$\dot{m}_d$	X_b	A_{ev}	A_{FWH}
1	65.0	64.5	60.0	60.0	240	8.5	232	8.5	44	1,640	0
2	62.7	62.2	65.0	57.7	232	8.5	223	17.0	45	3,380	164
3	60.5	59.9	62.7	55.5	223	8.5	215	25.4	47	3,400	165
4	58.2	57.6	60.5	53.2	215	8.5	206	33.8	49	3,430	165
5	55.9	55.3	58.2	50.9	206	8.5	198	42.2	51	3,470	166
6	53.6	53.0	55.9	48.6	198	8.5	190	50.6	53	3,510	166
7	51.4	50.7	53.6	46.4	190	8.5	181	58.9	56	3,550	167
8	49.1	48.4	51.4	44.1	181	8.5	173	67.2	58	3,600	168
9	46.8	46.1	49.1	41.8	173	8.5	165	75.4	61	3,650	168
10	44.6	43.8	46.8	39.6	165	8.5	156	83.6	64	3,720	169
11	42.3	41.5	44.6	37.3	156	8.5	148	91.8	68	3,790	170
12	40.0	39.2	42.3	35.0	148	8.5	140	100	72	3,880	171

Table 3
Parallel-cross MED results. 12 effects, PR = 10.3, SA = 524 $m^2/(kg/s)$, and area of down condenser = 902 m^2

Effect	T_b	T_d	T_f	$T_{i,FWH}$	$\dot{m}_f$	$\dot{m}_v$	$\dot{m}_b$	$\dot{m}_d$	X_b	A_{ev}	A_{FWH}
1	65.0	64.1	60.0	60.0	22.9	9.5	13.4	9.5	72	1,510	0
2	62.7	61.8	57.7	57.7	22.4	9.3	26.5	18.8	72	5,490	17
3	60.5	59.5	55.5	55.5	21.8	9.1	39.3	27.8	72	5,250	33
4	58.2	57.3	53.2	53.2	21.3	8.9	51.8	36.6	72	5,030	49
5	55.9	55.0	50.9	50.9	20.8	8.8	64.0	45.3	72	4,810	65
6	53.6	52.8	48.6	48.6	20.3	8.6	75.8	53.7	72	4,600	80
7	51.4	50.5	46.4	46.4	19.8	8.4	87.4	61.9	72	4,410	94
8	49.1	48.3	44.1	44.1	19.3	8.2	98.8	69.9	72	4,220	108
9	46.8	46.0	41.8	41.8	18.8	8.1	110	77.7	72	4,040	122
10	44.6	43.7	39.6	39.6	18.4	7.9	121	85.3	72	3,860	135
11	42.3	41.5	37.3	37.3	17.9	7.8	131	92.7	72	3,700	148
12	40.0	39.2	35.0	35.0	16.2	7.6	140	100	72	3,540	160

Table 4
Forward to parallel-cross MED results. 12 effects with transition at effect 6. PR = 10.2, SA = 490 $m^2/(kg/s)$, and area of down condenser = 919 m^2

Effect	T_b	T_d	T_f	$T_{i,FWH}$	$\dot{m}_f$	$\dot{m}_v$	$\dot{m}_b$	$\dot{m}_d$	X_b	A_{ev}	A_{FWH}
1	65.0	64.4	60.0	60.0	107	8.9	97.2	8.9	46	1,530	0
2	62.7	62.1	65.0	57.7	97.8	8.9	88.3	17.8	50	3,850	73
3	60.5	59.8	62.7	55.5	88.9	8.9	79.5	26.6	56	3,980	74
4	58.2	57.4	60.5	53.2	80.0	8.9	70.6	35.4	63	4,150	75
5	55.9	55.0	58.2	50.9	71.2	8.9	61.9	44.2	72	4,390	76
6	53.6	52.8	48.6	48.6	20.7	8.7	12.2	52.8	72	4,760	78
7	51.4	50.5	46.4	46.4	20.2	8.6	12.0	61.1	72	4,500	93
8	49.1	48.3	44.1	44.1	19.7	8.4	11.8	69.3	72	4,310	107
9	46.8	46.0	41.8	41.8	19.2	8.2	11.5	77.3	72	4,120	121
10	44.6	43.8	39.5	39.5	18.7	8.1	11.3	85.0	72	3,950	134
11	42.3	41.5	37.3	37.3	18.3	7.9	11.1	92.6	72	3,780	147
12	40.0	39.2	35.0	35.0	16.5	7.8	10.9	100	72	3,620	160

setting the brine salinity after flashing in the PC section (effects N_s to N_t) to the maximum brine salinity. In addition, the feed that is directed to the FF section (effects 1 to $N_s - 1$) is determined such that the outlet brine salinity in effect $(N_s - 1)$ is equal to the maximum brine salinity. Therefore, the RR is the same as the FF-MED and PC-MED cases.

Table 4 shows simulation results of the FF-PC-MED configuration with twelve effects. The configuration transitions to PC at the sixth effect. The PR is 10.2 and the specific surface area is 490 $m^2/(kg/s)$. As expected, the PR and the SA are intermediate values to that of FF-MED and PC-MED. Comparing against the linear combination of FF-MED or PC-MED is necessary; for a fixed PR, the FF-PC-MED configuration should have a lower SA than the linear combination of FF-MED and PC-MED SAs. Given that the FF-PC-MED PR is 84.5% of the difference between the FF-MED and PC-MED systems, the SA of the linear combination is 511 $m^2/(kg/s)$ for a PR of 10.18. The SA of the FF-PC-MED simulation is less than the linear combination SA by $\approx 4\%$. Therefore, a performance advantage exists for the FF-PC-MED configuration as compared to the fleet-average of FF-MED or PC-MED alone.

Fig. 5(a) shows the change in the performance of FF-PC-MED with varying number of effects, N_t, and transition effect, N_s. Fig. 5(b) shows the variation in number of effects from eight to thirteen with fixed operating conditions. Overall, the trend with increasing number of effects is nearly linear. For a fixed number of effects, however, the performance varies nonlinearly with FF-MED at the lowest PR and SA and PC-MED at the highest PR and SA with FF-PC-MED performance in between. For a fixed number of effects, all FF-PC-MED results are better (lower SA for a given PR) than the linear combination of the FF-MED and PC-MED results.

The performance shows a strong dependence on number of effects, as expected. However, an interesting result occurs at higher number of effects; the performance between two effects overlaps. Fig. 5(b) shows this outcome between twelve and thirteen effects. This overlap shows an advantage in performance for the FF-PC-MED configuration. Although PC-MED exhibits the highest PR and SA among twelve effect options, the thirteen effect FF-PC-MED with transition at effect ten has a higher PR ($\approx$0.18 points higher) with a lower SA ($\approx$7 $m^2/(kg/s)$ lower). Similarly, the twelve effect FF-PC-MED with transitions at six and seven effects exhibit greater PR and lower SA than the thirteen effect FF-MED.

The FF-PC-MED configuration is a promising alternative to either FF-MED or PC-MED. However, the analysis performed herein does not imply optimality since operating conditions are held fixed. Further, the models utilized are simplified and more accurate models are required for quantitative conclusions. The pumping requirements should also be compared, a measure of operating costs, among the configurations. Despite the limitations of the analysis performed herein, the demonstrated performance of the FF-PC-MED configuration shows that this hybrid thermal–thermal desalination concept has merit and should be further explored through detailed modeling and numerical optimization.

4.2. Simulation and discussion of MSF-MED

The performance of the MSF-MED concept is simulated with fixed operating conditions and total

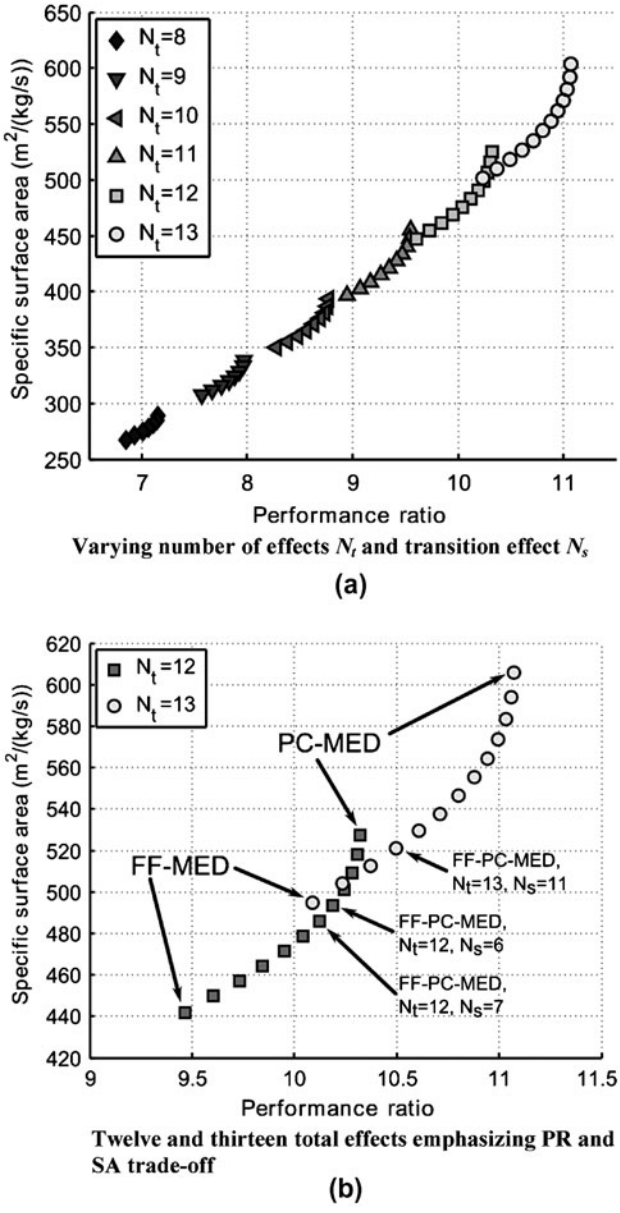

Fig. 5. Performance of FF-PC-MED (Fig. 1) configuration with varying number of effects and transition effects.

number of units (24 stages/effects) in order to constrain capital expenditures. Table 5 shows the operating parameters considered; a linear temperature profile is assumed. In this configuration, the TBT is the temperature at the outlet of the brine heater (typical of MSF configurations). Therefore, the temperature difference between each unit is given by:

$$\Delta T = \frac{TBT - T_{bd}}{N_t}$$

The transition unit, N_s, where the configuration switches from MSF to MED is considered variable

Table 5
Operating parameters for MSF-MED (Fig. 2) and MSF-OT configuration

Unit distillate flow (kg/s)	100
Seawater temperature (℃)	25
Seawater salinity (g/kg)	42
Max. brine salinity (g/kg)	72
Steam supply temp., saturated (℃)	116
Top brine temp., TBT (℃)	105
Brine blowdown temp., T_{bd} (℃)	35
Total number of units, N_t	24

given the constraint that the MED effects should not be operated at a brine temperature above ≈70℃ in order to avoid scaling. Therefore, given a linear temperature profile with twenty-four units, the transition unit must be greater or equal to unit twelve ($N_s \leq 12$). In this configuration, the feed flowrate cannot simultaneously maximize RR while satisfying the distillate production requirement since the external steam source is used only for heating feed. Therefore, the recovery of this system is rather low.

Table 6 shows the performance of the MSF-MED concept for 24 total units with a transition unit of 12. The system achieves a PR of 9.75 with an SA of 238 $m^2/kg/s$) and a recovery ratio of 17.6%. The amount of vapor produced in unit 11 (powering the MED section) is approximately 30% of the steam necessary to power the twelve effect FF-MED system investigated in Section 4.1. Therefore, a significant amount of distillate can be generated by utilizing the enthalpy of vaporization of flashed vapors to power film boiling as opposed to feedwater heating. From the values of $\dot{m}_d$ the total flow of distillate leaving each effect/stage, it can be seen that the MED section produces about 70% of the total distillate generated. The PR of the MED section alone is significantly higher than the FF-MED system because of gained enthalpy of the incoming MSF brine. In addition, this system is operated at a lower brine blowdown temperature without cooling seawater for fair comparison to the typical operating conditions of once-through MSF.

Fig. 6 shows PR vs. SA results of the MSF-MED system with fixed operating conditions and total number of units for varying transition unit N_s. The simulated performance of MSF-OT for twenty-four stages is also shown; the recovery of the MSF-OT system is 11.3%. Fig. 6 shows that the transition to MED effects increases the PR and the SA, as expected. As compared to the FF-MED system in Section 4.1, the SA is significantly less for a similar PR. However, the steam supply temperature is much higher in the MSF-MED case, the RR is less, and there is no cooling

Table 6
MSF-MED results for $N_t = 24$ with transition unit $N_s = 12$. PR = 9.75, SA = 238 $m^2/(kg/s)$, and RR = 17.6%

Effect	T_b	T_d	T_f	$T_{i,FWH}$	$T_{o,FWH}$	$\dot{m}_f$	$\dot{m}_v$	$\dot{m}_b$	$\dot{m}_d$	X_b	A_{ev}	A_{FWH}
1	102	101	105	95.0	105	567	2.8	564	2.8	42	0	610
2	99.2	98.5	102	82.1	95.0	564	2.8	561	5.7	42	0	353
3	96.3	95.6	99.2	89.2	92.1	561	2.8	558	8.5	43	0	352
4	93.3	92.7	96.3	86.2	89.2	558	2.8	556	11.3	43	0	352
5	90.4	89.8	93.3	83.3	86.2	556	2.8	553	14.0	43	0	352
6	87.5	86.9	90.4	80.4	83.3	553	2.8	550	16.8	43	0	351
7	84.6	84.0	87.5	77.5	80.4	550	2.8	547	19.5	44	0	351
8	81.7	81.1	84.6	74.6	77.5	547	2.8	545	22.3	44	0	351
9	78.8	78.2	81.7	71.7	74.6	545	2.8	542	25.0	44	0	350
10	75.8	75.3	78.8	68.7	71.7	542	2.8	539	27.7	44	0	350
11	72.9	72.3	75.8	65.8	68.7	539	2.8	537	30.4	44	0	350
12	70.0	69.4	72.9	65.8	65.8	537	5.7	531	35.9	45	939	0
13	67.1	66.5	70.0	62.9	65.8	531	5.7	526	41.4	45	937	560
14	64.2	63.6	67.1	60.0	62.9	526	5.7	520	46.9	46	935	559
15	61.2	60.7	64.2	57.1	60.0	520	5.7	515	52.3	46	933	559
16	58.3	57.8	61.3	54.2	57.1	515	5.7	509	57.7	47	932	558
17	55.4	54.9	58.3	51.2	54.2	509	5.7	504	63.1	47	930	558
18	52.5	52.0	55.4	48.3	51.2	504	5.7	449	68.5	48	928	557
19	49.6	49.1	52.5	45.4	48.3	449	5.7	493	73.8	48	926	556
20	46.7	46.1	49.6	42.5	45.4	493	5.7	488	79.1	49	924	556
21	43.8	43.2	46.7	39.6	42.5	488	5.7	483	84.4	49	922	555
22	40.8	40.3	43.8	36.7	39.6	483	5.7	477	89.6	50	920	555
23	37.9	37.4	40.8	33.7	36.7	477	5.7	472	94.8	50	918	554
24	35.0	34.5	37.9	30.8	33.7	472	5.7	467	100	51	916	554

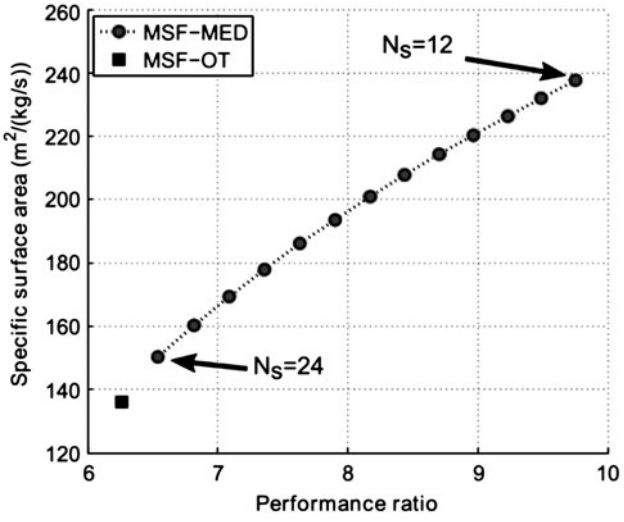

Fig. 6. Performance of MSF-MED concept as compared to MSF-OT for fixed operating conditions and total number of units ($N_t = 24$) with varying transition unit from $N_s = 12$ to $N_s = 24$.

water stream to buffer against changes in seawater temperature [43].

Table 7
Operating parameters for FF-MED-TVC, PC-MED-TVC, and MSF-MED-TVC (Fig. 3) configurations

Unit distillate flow (kg/s)	100
Seawater temperature (℃)	25
Seawater salinity (g/kg)	42
Max. brine salinity (g/kg)	72
Steam supply temp., saturated (℃)	116
Top brine temp., TBT (℃)	105
Brine blowdown temp., T_{bd} (℃)	40
Condenser temp. (℃)	35
Number of MSF stages, $N_{t,MSF}$	15
Number of MED effects, $N_{t,MED}$	12

Despite the limitations of the concept shown herein, feed/brine extraction or mixing could possibly be utilized in order to increase recovery. Utilizing a variation of the MSF-MED concept could result in a higher PR vs. SA as compared to FF-MED or MSF-BR (not compared herein due to differences in operating conditions). In addition, the alternate construct of condensing flashed vapors inside of tubes should be further investigated through detailed heat transfer

models to account for changes in heat transfer coefficient as compared to a typical MSF stage or MED effect.

4.3. Simulation and discussion of MSF-MED-TVC

To simulate the performance of the MSF-MED-TVC system, the steam supply conditions, blowdown conditions, and number of stages/effects are held fixed. Table 7 shows the operating parameters considered herein. The TVC compression ratio, MSF last stage brine temperature, and MED TBT are considered variable. Since the motive steam and blowdown temperatures are held fixed, varying the CR of the TVC changes the discharge saturation temperature of the TVC. The MED TBT and MSF last stage brine temperature are fixed with respect to the discharge conditions. The difference in temperature between the TVC discharge temperature and the MED TBT is set as 4℃, and the difference in temperature between the MSF last stage brine temperature and MED TBT is set as 1℃. These values ensure that reasonable pinches exist in the feedwater heaters and MED effects.

Table 8
Variation of TVC compression ratio for $P_{m,sat} = 0.175$ MPa ($T_{m,sat} = 116$℃) and $P_{e,sat} = 0.00732$ MPa ($T_{e,sat} = 40$℃), with resulting entrainment ratio, discharge temperature, MED TBT, and MSF last effect brine temperature

CR	ER	$T_{sat,di}$ (℃)	TBT_{MED} (℃)	$T_{b,Nt}$ (℃)
3	2.31	62.3	58.3	59.3
3.5	2.77	65.7	61.7	62.7
4	3.25	68.7	64.7	65.7
4.5	3.74	71.5	67.5	68.5
5	4.23	73.9	69.9	70.9

Table 8 shows the considered compression ratios and the resulting entrainment ratio and operating temperatures given the steam supply and blowdown conditions that are assumed herein. A linear brine temperature profile is assumed between the MSF TBT and MSF last stage brine temperature; similarly, a

Table 9
MSF-MED-TVC results for MSF $N_t = 15$ and MED $N_t = 12$, and CR = 4. PR = 13.0, and SA = 418.1 $m^2/(kg/s)$

Effect/stage	T_b	T_d	T_f	$T_{i,FWH}$	$T_{o,FWH}$	$\dot{m}_f$	$\dot{m}_v$	$\dot{m}_b$	$\dot{m}_d$	X_b	A_{ev}	A_{FWH}
MSF 1	102	102	105	99.0	105	240	1.08	239	1.08	42	0	174
MSF 2	99.8	99.1	102	96.4	99.0	239	1.08	238	2.15	42	0	268
MSF 3	97.1	96.5	99.8	93.8	96.4	238	1.08	237	3.22	43	0	268
MSF 4	94.5	93.9	97.1	91.1	93.8	237	1.08	236	4.28	43	0	267
MSF 5	91.9	91.3	94.5	88.5	91.1	236	1.08	235	5.34	43	0	267
MSF 6	89.3	88.7	91.9	85.9	88.5	235	1.08	234	6.39	43	0	266
MSF 7	86.7	86.1	89.3	83.3	85.9	234	1.08	233	7.44	43	0	266
MSF 8	84.1	83.5	86.7	80.7	83.3	233	1.08	232	8.48	44	0	265
MSF 9	81.4	80.9	84.1	78.1	80.7	232	1.08	230	9.52	44	0	265
MSF 10	78.8	78.2	81.4	75.4	78.1	231	1.08	229	10.6	44	0	264
MSF 11	76.2	75.6	78.8	72.8	75.4	229	1.08	228	11.6	44	0	264
MSF 12	73.6	73.0	76.2	70.2	72.8	228	1.08	227	12.6	44	0	264
MSF 13	71.0	70.4	73.6	67.6	70.2	227	1.08	226	13.6	45	0	263
MSF 14	68.4	67.8	71.0	65.0	67.6	226	1.08	225	14.6	45	0	263
MSF 15	65.7	65.2	68.4	62.4	65.0	225	1.08	224	15.7	45	0	262
MED 1	64.7	64.2	65.7	59.7	59.7	224	7.20	217	24.4	46	1,320	0
MED 2	62.5	61.9	64.7	57.5	59.7	218	7.21	210	31.5	48	2,900	164
MED 3	60.2	59.6	62.5	55.2	57.5	210	7.22	203	38.6	50	2,930	165
MED 4	58.0	57.4	60.2	53.0	55.2	203	7.22	196	45.7	51	2,960	165
MED 5	55.7	55.1	58.0	50.7	53.0	196	7.23	189	52.7	53	2,990	165
MED 6	53.5	52.9	55.7	48.5	50.7	189	7.24	182	59.8	55	3,020	166
MED 7	51.2	50.6	53.5	46.2	48.5	182	7.25	175	66.8	58	3,060	166
MED 8	49.0	48.3	51.2	44.0	46.2	175	7.25	168	73.8	60	3,100	167
MED 9	46.7	46.0	49.0	41.7	44.0	168	7.26	161	80.7	63	3,140	168
MED 10	44.5	43.8	46.7	39.5	41.7	161	7.27	154	87.7	66	3,190	168
MED 11	42.2	41.5	44.5	37.2	39.5	154	7.28	147	94.6	69	3,250	169
MED 12	40.0	39.2	42.2	35.0	37.2	147	7.29	140	100	72	3,320	170

linear brine temperature profile is assumed (not necessarily equal to the MSF section) between the MED TBT and MED last stage brine temperature (T_{bd}). The total feed flowrate is chosen such that the MED last effect blowdown salinity is the maximal allowable salinity (72 g/kg). Table 9 shows the resulting performance of the MSF-MED-TVC concept for TVC CR = 4. The system achieves a PR of 13.0 and SA of 418 $m^2/(kg/s)$.

It is necessary to compare this configuration's performance vs. standard configurations. Specifically, FF-MED-TVC and PC-MED-TVC are considered. The motivation behind comparing with FF-MED-TVC is to determine if the addition of the MSF section (with the same MED section configuration as FF-MED-TVC) constitutes a gain in performance with respect to PR or SA. Based on the results of Section 4.1, the PC-MED-TVC configuration exhibits higher PR and SA for fixed operating conditions as compared to FF-MED-TVC. Therefore, if the MSF-MED-TVC concept exhibits a gain in performance as compared to FF-MED-TVC, it is important to weigh this difference with respect to the PC-MED-TVC configuration.

The performance of FF-MED-TVC and PC-MED-TVC is simulated with the same MED section operating conditions shown in Table 7. For fixed number of effects (N_t=12), the TBT is varied by the TVC CR (based on Table 8). Fig. 7 shows the resulting MSF-MED-TVC, FF-MED-TVC, and PC-MED-TVC performance for varying CR and fixed number of stages/effects. For MSF-MED-TVC, the number of MSF stages is 15, and the number of MED effects is 12. The SA for each configuration increases with decreasing CR, i.e., MED TBT, because the number of effects is fixed and therefore the feedwater heater and effect pinches decrease. However, the PR increases for decreasing CR, mostly due to the decrease in entrainment ratio, i.e., less motive steam is needed for the same vapor drawn from the last effect of MED.

Fig. 7 demonstrates that the MSF-MED-TVC concept exhibits a higher PR and lower SA as compared to FF-MED-TVC for all CR tested. However, the MSF-MED-TVC shows a lower PR and lower SA as compared to PC-MED-TVC for a given CR. On the other hand, for all CR considered, the MSF-MED-TVC follows a similar performance trend as PC-MED-TVC. The performance of the MSF-MED-TVC concept as compared to the FF-MED-TVC configuration indicates that there is merit in the addition of high-temperature MSF stages in combination with MED-TVC. Again, as with the other concepts studied, more detailed modeling is necessary in order to fully determine the performance gains possible with the MSF-MED-TVC concept. Further, a scheme that integrates a PC-MED section as opposed to a FF-MED section could perhaps exhibit better performance in comparison to PC-MED-TVC alone. Another configuration possibility is the use of a low-pressure steam supply to power the MED section without utilizing TVC. This configuration could have an advantage in reducing lost work of power production.

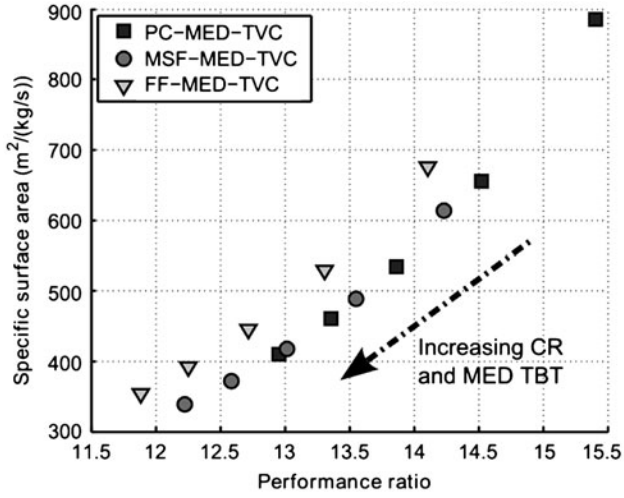

Fig. 7. Performance of MSF-MED-TVC concept as compared to FF-MED-TVC and PC-MED-TVC with varying TVC compression ratio and fixed number of stages/effects.

5. Conclusion

In this article, hybrid thermal–thermal desalination concepts are proposed, and their performance vs. standard thermal desalination configurations is investigated. The studied configurations are the following (i) FF-PC-MED: a configuration which transitions from FF-MED effects to PC-MED effects (FF-PC-MED-TVC is also possible, but not analyzed herein); (ii) MSF-MED: a configuration which transitions from MSF stages to FF-MED effects and features an alternative MSF stage type; (iii) MSF-MED-TVC: a configuration which uses parallel steam supplies to power an MSF section and MED-TVC section operating in series.

Each of these configurations are evaluated in terms of their PR, SA, and RR and are promising alternatives to standard thermal desalination configurations. The FF-PC-MED system exhibits a lower SA than the linear combination of standalone FF-MED and PC-MED SA for a given PR and fixed operating conditions and number of effects. This metric indicates better performance as compared to the standalone systems. The MSF-MED concept exhibits higher RR and PR as compared to MSF-OT for fixed operating conditions and number of effects/stages. The RR of the

MSF-MED concept could be improved with use of brine recirculation. Finally, the MSF-MED-TVC concept exhibits a higher PR and lower SA as compared to FF-MED-TVC alone for fixed number of effects and MED-TVC operating range.

However, the simulation of these concepts does not utilize rigorous modeling or numerical optimization. Therefore, substantial future work is necessary to determine the full performance improvement of these concepts. This work should include the use of nonconstant physical properties and heat transfer coefficients as well as the calculation of pumping requirements and the effect of demisters, noncondensable gases, de-superheaters, fouling resistances, and/or nonequilibrium allowance on performance similar to [28]. These detailed models will be utilized to perform numerical optimization of the design and operation of these systems as well as standard thermal desalination configurations. In order to fairly compare the potential of each system vs. standard configurations, optimized performance results must be utilized. The models will likely be highly nonconvex; therefore, in principle, global optimization should be used. It is also necessary to consider the simultaneous maximization of PR and RR and minimization of SA through multi-objective optimization.

Acknowledgements

The authors would like to thank the King Fahd University of Petroleum and Minerals in Dhahran, Saudi Arabia, for funding this work through the Center for Clean Water and Clean Energy at MIT and KFUPM under project number R13-CW-10. The authors also thank Numerica Technology for providing access to JACOBIAN software utilized for this research. Finally, the authors thank Professor John H. Lienhard V for thoughtful discussions and input regarding the work herein.

Symbols

A	—	area, m^2
c_p	—	specific heat capacity, kJ/(kg K)
$\dot{m}$	—	flowrate, kg/s
h	—	specific enthalpy, kJ/kg
Δh_{fg}	—	enthalpy of vaporization, kJ/kg
P	—	pressure, kPa
$\dot{Q}$	—	thermal power, kW
SA	—	specific area, $m^2/(kg/s)$
T	—	temperature, ℃
U	—	overall heat transfer coefficient, $kW/(m^2K)$
X	—	salinity, g/kg

Abbreviations

BPE	—	boiling point elevation
BR	—	brine-recirculating (MSF)
CR	—	compression ratio
ER	—	entrainment ratio
FF	—	forward-feed (MED)
FWH	—	feedwater heater
MED	—	multi-effect distillation
MSF	—	multi-stage flash
N	—	effect/stage
OT	—	once-through (MSF)
PC	—	parallel-cross (MED)
PR	—	performance ratio
RR	—	recovery ratio
TBT	—	top brine temperature
TVC	—	thermal vapor compression

Subscripts

b	—	brine
bd	—	(brine) blowdown
d	—	distillate
di	—	discharge stream (TVC)
e	—	entrained stream (TVC)
ev	—	evaporation
f	—	feed
i	—	inlet
m	—	motive stream (TVC)
o	—	outlet
q	—	associated with heat transfer
s	—	transition (effect/stage)
t	—	total number (of effects/stages)
v	—	vapor

References

[1] H. El-Dessouky, I. Alatiqi, H. Ettouney, Process synthesis: The multi-stage flash desalination system, Desalination 115(2) (1998) 155–179.
[2] M.A. Darwish, H.K. Abdulrahim, Feed water arrangements in a multi-effect desalting system, Desalination 228(1–3) (2008) 30–54.
[3] A.O. Bin Amer, Development and optimization of ME-TVC desalination system, Desalination 249(3) (2009) 1315–1331.
[4] N.M. Abdel-Jabbar, H.M. Qiblawey, F.S. Mjalli, H. Ettouney, Simulation of large capacity MSF brine circulation plants, Desalination 204(1–3) (2007) 501–514.
[5] A. Ophir, F. Lokiec, Advanced MED process for most economical sea water desalination, Desalination 182(1–3) (2005) 187–198.
[6] G. Kronenberg, F. Lokiec, Low-temperature distillation processes in single- and dual-purpose plants, Desalination 136(1–3) (2001) 189–197.
[7] M. Al-Sahali, H. Ettouney, Developments in thermal desalination processes: Design, energy, and costing aspects, Desalination 214(1–3) (2007) 227–240.

[8] A. Nafey, H. Fath, A. Mabrouk, Thermo-economic investigation of multi effect evaporation (MEE) and hybrid multi effect evaporation-multi stage flash (MEE-MSF) systems, Desalination 201(1–3) (2006) 241–254.
[9] H.T. El-Dessouky, H.M. Ettouney, Fundamentals of Salt Water Desalination, Elsevier, Amsterdam, 2002.
[10] C. Sommariva, N. Lior, E. Sciubba, D. Pinciroli, Innovative configuration for multi stage flash desalination plant, in: IDA proceedings, San Diego, vol. I, 1999, p. 16.
[11] C. Sommariva, Novel hybrid MED-MSF concept: Increasing efficiency and production in combined power and desalination plants, in: IDA World Congress, Singapore, 2005.
[12] C. Sommariva, L. Awerbuch, Improving efficiencies in thermal desalination systems: The Layyah plant experience, in: International Water Forum Dubai, 2006.
[13] L. Awerbuch, C. Sommariva, Future challenges of integration of desalination, power, energy, environment, and security, in IDA World Congress, Gran Canaria, Spain, 2007.
[14] S.F. Mussati, P.A. Aguirre, N.J. Scenna, Novel configuration for a multistage flash-mixer desalination system, Ind. Eng. Chem. Res. 42(20) (2003) 4828–4839.
[15] S.F. Mussati, P.A. Aguirre, N.J. Scenna, Improving the efficiency of the MSF once through (MSF-OT) and MSF-mixer (MSF-M) evaporators, Desalination 166 (2004) 141–151.
[16] S.F. Mussati, P.A. Aguirre, N.J. Scenna, Superstructure of alternative configurations of the multistage flash desalination process, Ind. Eng. Chem. Res. 45(21) (2006) 7190–7203.
[17] N.J. Scenna, Synthesis of thermal desalination processes. Part I. Multistage flash distillation system (MSF), Desalination 64 (1987) 111–122.
[18] N.J. Scenna, Synthesis of thermal desalination processes. Part II. Multi effect evaporation, Desalination 64 (1987) 123–135.
[19] G.M. Zak, Thermal desalination: Structural optimization and integration in clean power and water, Master's thesis, Massachusetts Institute of Technology, 2012.
[20] A. Nafey, H. Fath, A. Mabrouk, Exergy and thermoeconomic evaluation of MSF process using a new visual package, Desalination 201(1–3) (2006) 224–240.
[21] H.T. El-Dessouky, H.M. Ettouney, Multiple-effect evaporation desalination systems. Thermal analysis, Desalination 125(1–3) (1999) 259–276.
[22] M.A. Darwish, F. Al-Juwayhel, H.K. Abdulraheim, Multi-effect boiling systems from an energy viewpoint, Desalination 194(1–3) (2006) 22–39.
[23] K.S. Spiegler, Principles of desalination, second ed., Academic Press, New York, NY, 1980.
[24] N.D. Mancini, A. Mitsos, Conceptual design and analysis of ITM oxy-combustion power cycles, Phys. Chem. Chem. Phys. 13(48) (2011) 21351–21361.
[25] E.J. Sheu, A. Mitsos, A.A. Eter, E.M.A. Mokheimer, M.A. Habib, A. Al-Qutub, A review of hybrid solar-fossil fuel power generation systems and performance metrics, ASME J. Solar Energy Eng. 134(4) (2012) 041006:1–17.
[26] F. Rahman, Z. Amjad, Scale formation and control in thermal desalination systems, in: The Science and Technology of Industrial Water Treatment, CRC Press, Brecksville, OH, 2010, pp. 271–396.
[27] M.M. Ashour, Steady state analysis of the Tripoli West LT-HT-MED plant, Desalination 152(1–3) (2003) 191–194.
[28] K. Mistry, M.A. Antar, J.H. Lienhard, An improved model for multiple effect distillation, Desalination and Water Treatment 51 (2012) 807–821.
[29] H.T. El-Dessouky, H.M. Ettouney, Multiple Effect Evaporation, in: Fundamentals of Salt Water Desalination, Elsevier, Amsterdam, 2002, pp. 147–208.
[30] M.S. Tanvir, I.M. Mujtaba, Optimisation of design and operation of MSF desalination process using MINLP technique in gPROMS, Desalination 222(1–3) (2008) 419–430.
[31] H.E.S. Fath, The non-equilibrium factor and the flashing evaporation rate inside the flash chamber of a multi-stage flash desalination plant, Desalination 114(3) (1997) 277–287.
[32] H. El-Dessouky, Modelling and simulation of the thermal vapour compression desalination process, in: Nuclear Desalination of Seawater, International Atomic Agency, 1997, pp. 315–338.
[33] H. Sayyaadi, A. Saffari, Thermoeconomic optimization of multi effect distillation desalination systems, Appl. Energy 87(4) (2010) 1122–1133.
[34] H. Sayyaadi, A. Saffari, A. Mahmoodian, Various approaches in optimization of multi effects distillation desalination systems using a hybrid meta-heuristic optimization tool, Desalination 254(1–3) (2010) 138–148.
[35] N.H. Aly, A.K. El-Fiqi, Thermal performance of seawater desalination systems, Desalination 158 (2003) 127–142.
[36] K. Spiegler, Y. El-Sayed, A Desalination Primer, Balaban Desalination Publications, Santa Maria, 1994.
[37] International Association for the Properties of Water and Steam, Revised Release on the IAPWS Industrial Formulation 1997 for the Thermodynamic Properties of Water and Steam, 2007.
[38] M.H. Sharqawy, J.H. Lienhard, S.M. Zubair, Thermophysical properties of seawater: A review of existing correlations and data, Desalin. Water Treat. 16(1–3) (2010) 354–380.
[39] F.P. Incropera, Fundamentals of Heat and Mass Transfer, sixth ed., John Wiley, Hoboken, NJ, 2007.
[40] B. Huang, J. Chang, C. Wang, V. Petrenko, A 1-D analysis of ejector performance, Int. J. Refrigeration-Rev. Int. Du Froid 22(5) (1999) 354–364.
[41] Numerica Technology, JACOBIAN Modeling and Optimization Software, Cambridge, MA, 2009.
[42] K. Ansari, H. Sayyaadi, M. Amidpour, Thermoeconomic optimization of a hybrid pressurized water reactor (PWR) power plant coupled to a multi effect distillation desalination system with thermo-vapor compressor (MED-TVC), Energy 35(5) (2010) 1981–1996.
[43] H. Ettouney, H. El-Dessouky, F. Al-Juwayhel, Performance of the once-through multistage flash desalination process, Proc. Institution Mech. Eng. Part A – J. Power Energy 216(A3) (2002) 229–241.